

# Topology of Charge Density from Pseudopotential Density Functional Theory Calculations

Nawzat Saeed Saadi

School of Physics , Duhok University, Duhok, Kurdistan Region, Iraq

\* E-mail of the corresponding author: [nawzat@uod.ac](mailto:nawzat@uod.ac)

## Abstract

The absence of core electrons in pseudopotential electronic structure calculations poses some important problems on determining the topology of density. The key feature of valence-only densities is the lack of critical points (CPs) at the nuclear positions affected by core removal, which are sometimes substituted by local minimum CPs, the substitution of a maximum by a minimum must be necessarily accompanied by the creation of other compensating CPs, including at least either one maximum or one ring CP. As density is relatively unaffected at distance points far enough the removed cores, these new CPs are expected to lie in the proximity of the latter, and the topology of density to closely resemble that of the AE density in the chemically relevant valence regions. This difficulty is well-known in literature, and several works have been devoted to elucidate how to bypass it (Cioslowski and Piskorz, 1996). The correct topologies may be obtained from core-reconstructed pseudo-AE densities. This paper will show how the correct topology can be obtained from pseudopotential calculations. In order to analyze the problems that arise from the core electrons, results obtained for Alanine ( $\text{CH}_3\text{CH}(\text{NH}_2)\text{COOH}$ ), Aminophenol ( $\text{C}_6\text{H}_4(\text{OH})\text{NH}_2$ ), Ethene ( $\text{C}_2\text{H}_4$ ), and Propanone ( $(\text{CH}_3)_2\text{CO}$ ) using all-electron, pseudo-valence wavefunctions are reported.

**Keywords:** Pseudopotential, core electrons, all-electron (AE) density, QTAIM, charge density topology.

## 1. Introduction

Pseudopotential (PP) techniques allow core electrons removal. Valence electrons then move in a smoother (nonlocal) potential in core region and exhibit a behavior same as in an all-electron outside the core. Using pseudopotentials in electronic structure calculations would contribute in numerical advantages when solving Kohn-Sham equations and reduce the time required for calculations. On the other hand, the absence of cores has an obvious drawback within the Quantum Theory of Atoms in Molecules (QTAIM), Electron density  $n(\mathbf{r})$  constructed from pseudo-valence orbitals lacks the maxima (cusps) at the nuclear positions that define the atomic basins. This means that despite PP energetics is well-behaved, the topology of the valence-only density  $n_{\text{val}}(\mathbf{r})$  may be completely different from that obtained with the all-electron (AE) density  $n_{\text{AE}}(\mathbf{r})$  (Phillips and Kleinman, 1959).

## 2. Atomic charges, atomic charge analysis schemes and packages

Atomic charges in molecules or solids are not observables and, therefore not defined by quantum mechanics theory. The output of quantum mechanics calculations is continuous electronic charge density and it is not clear how one should partition electrons amongst fragments of the system such as atoms or molecules.

There are many ways to partition the total net charge of a molecule into the charges of the atoms composing the molecule, but the most three commonly used methods are (Jensen, 2006): Partitioning the wavefunction in terms of the basis functions, Fitting schemes, and Partitioning the electron density into atomic domains.

Analysis based on basis functions include Mulliken population analysis, which is one of the oldest and still most frequently cited charge decomposition schemes. This can be a fast and useful way of determining partial charges on atoms, but it has the major drawback that the analysis is sensitive to the choice of basis set (Mulliken, 1955).

Analysis based on the electron density include Bader (Bader, 1994), Voronoi (Rousseau, Peeters and Alsenoy, 2001), Hirshfeld (Hirshfeld, 1977), and Stewart charge analysis scheme (Fonseca Guerra et al., 2004). Perhaps the most rigorous way of dividing a molecular volume into atomic subspaces is QTAIM developed by R. Bader, in Bader analysis the space is divided into regions by surfaces that run through minima in the charge density (Bader, 1994).

Analysis based on the electrostatic potential is one area where the concept of atomic charges is deeply rooted in force field methods. A significant part of the non-bonded interaction between polar molecules is described in terms of electrostatic interactions between fragments having an internal asymmetry in the electron distribution.

The fundamental interaction is between Electrostatic Potential (ESP) (also called the Molecular Electrostatic Potential (MEP)) generated by one molecule (or fraction thereof) and the charged particles of another (Francl and Chirlian, 2007).

The InteGriTy package analyses experimentally obtained electron densities sampled on 3D grids. The accuracy of the topological analysis of electron densities grids has also been investigated. This approach depends on a careful interpolation of the electron density for the whole molecule or crystal (Katan et al., 2003). Critic2 is a topological analysis of solid state electron densities program. It applies a new algorithm for the integration of properties in atomic basins (de-la Roza et al., 2009). The TopMoD allows the calculation of the electron localization function (ELF) on a 3-dimensional grid, the assignment of the basins and the calculation of the basin populations, and of variance (Stephane et al., 1999). MORPHY, a program to perform topological analysis, is formulated by the theory of "Atoms in Molecules" (AIM) developed by Bader and co-workers (Bader, 1994). It can analyze wavefunction of a molecule or complex in terms of charge transfer, hydrogen bonding, electrostatic moments, bond topology, etc. (L.A. and Popelier, 1996). Recently, Henkelman et al. developed an on-grid method to divide an electron density grid into Bader volumes. This method can be applied to the DFT calculations of large molecules or materials. They discretize the trajectory to lie on the grid, ending at the local maximum point of the electron density. The points along each trajectory are assigned to the atom closest to the end point. This method is robust, and scales linearly with the grid size (Henkelman, Arnaldsson and J, 2006).

### 3. Quantum theory of atoms in molecules (QTAIM)

Bader's Quantum Theory of Atoms in Molecules (QTAIM) (Bader, 1994) is based on the assumption, that the properties of a molecule can be described as the sum of the properties of its atoms. Therefore, an unambiguous definition of an atom is compulsory. Mathematically, the density  $n(\mathbf{r})$  of a molecule is a scalar field and its topology is best examined by an analysis of its gradient vector field. The gradient is defined as:

$$\nabla n(\mathbf{r}) = \frac{\partial n}{\partial x} \hat{\mathbf{i}} + \frac{\partial n}{\partial y} \hat{\mathbf{j}} + \frac{\partial n}{\partial z} \hat{\mathbf{k}} \quad (1)$$

Here,  $\hat{\mathbf{i}}$ ,  $\hat{\mathbf{j}}$ , and  $\hat{\mathbf{k}}$  are the unit vectors of the cartesian coordinate system. A gradient path (also called trajectory) is always perpendicular to the contour lines of density and follows the largest increase in density. Therefore, it must originate from a minimum or saddle point (minimum in at least one direction) and terminate at a maximum or saddle point (maximum in at least one direction) of density. All trajectories ending at one maximum belong to the same basin, which represents an atom in a molecule. The definition of the atomic basins already contained another crucial element of Bader's QTAIM. The start and end points of a gradient path are extreme values in density. These extrema (maxima, saddle points, or minima in the electron density) all have a vanishing gradient of density. They are called critical points (CPs) and can be divided in core, bond, ring, and cage critical points, depending on the nature of the extremity. The inspection of the nature of the extremity can be performed with the help of the second order derivative of the density. The nine second order derivatives of  $n(\mathbf{r})$  form the Hessian matrix. In its diagonalized form (equation (2)), the Hessian matrix provides the three eigenvalues  $\lambda_1, \lambda_2$ , and  $\lambda_3$  (with  $\lambda_1 \leq \lambda_2 \leq \lambda_3$ ), which indicate the curvature of  $n(\mathbf{r})$  along the main curvature axes at the point  $r$ .

$$D(r_{CP}) = \begin{bmatrix} \frac{\partial^2 n(\mathbf{r})}{\partial x^2} & 0 & 0 \\ 0 & \frac{\partial^2 n(\mathbf{r})}{\partial y^2} & 0 \\ 0 & 0 & \frac{\partial^2 n(\mathbf{r})}{\partial z^2} \end{bmatrix} = \begin{bmatrix} \lambda_1 & 0 & 0 \\ 0 & \lambda_2 & 0 \\ 0 & 0 & \lambda_3 \end{bmatrix} \quad (2)$$

A critical point in  $n(\mathbf{r})$  is classified by the rank  $m$  (the number of non zero eigenvalues  $\lambda_i$ ) and the signature  $n$  (the algebraic sum of the signs of the eigenvalues  $\lambda_i$ ) of the Hessian matrix. For a rank  $m = 3$ , there are only four possible types of CPs with  $(m,n)$  (Table 1).

Table 1 Classification of critical points in  $n(\mathbf{r})$

(m, n)	Topology in $n(\mathbf{r})$	$\lambda_i$	Interpretation	Type
(3,-3)	local maximum	all $\lambda_i < 0$	atomic position	atom position (AP)
(3,-1)	maximum in two directions minimum in one direction	two $\lambda_i > 0$ one $\lambda_i < 0$	chemical bond	bond critical point (BCP)
(3,+1)	maximum in one direction minimum in two directions	one $\lambda_i > 0$ two $\lambda_i < 0$	centre of a ring of connected atoms	ring critical point (RCP)
(3,+3)	local minimum	all $\lambda_i > 0$	centre of a cube of connected atoms	cage critical point (CCP)

#### 4. Topology of density from pseudopotential calculations

The absence of core electrons in pseudopotential electronic structure calculations poses some important problems on determining the topology of density. The key feature of valence-only densities is the lack of (3,-3) critical points (CPs) at the nuclear positions affected by core removal, which are sometimes substituted by (3,+3) CPs. Since the Poincaré-Hopf (or Morse) topological invariant must retain its value and the indices of (3,-3) and (3,+3) CPs are of opposite sign, the substitution of a maximum by a minimum must be necessarily accompanied by the creation of other compensating CPs, including at least either one maximum or one (3,+1) ring CP. As density is relatively unaffected at  $\mathbf{r}$  points far enough from the removed cores, these new CPs are expected to lie in the proximity of the latter, and the topology of density to closely resemble that of the AE density in the chemically relevant valence regions. In their paper, Vyboishchikov (Vyboishchikov, Sierraalta and Frenking, 1997) showed that correct topologies may be obtained from core-reconstructed pseudo-AE densities. Hence review two different procedures. In the first, called augmented  $n_{aug}(\mathbf{r})$ , the pseudo-AE density is obtained adding a core density of single-atom AE core density  $n_{core}(\mathbf{r})$  (generated in an independent atomic calculation) to the coreless density  $n_{val}(\mathbf{r})$  obtained in a pseudopotential calculation:  $n_{aug}(\mathbf{r}) = n_{core}(\mathbf{r}) + n_{val}(\mathbf{r})$ . In the second, the core orbitals are orthogonalized to the valence ones, and the pseudo-AE density,  $n_{orth}(\mathbf{r})$  is derived from the orthogonalized determinant. On the other hand, one might encounter difficulties if the attached atomic core orbitals are not orthogonal to the valence molecular orbitals. Orthogonalized densities yielded no clear-cut improvement over either the local properties at critical points or the integrated ones over atomic basins. Indeed, atomic populations and bond orders were shown to worsen considerably with respect to AE values, this effect being traced to the diffuse tails induced in the core orbitals upon orthogonalization. Hence it was not considered.

#### 4.1 Electronic density and Density of an isolated atom

During the last five decades, an alternative way of looking at the quantum theory of atoms, molecules, and solids in terms of the electron density in three-dimensional (3D) space, rather than the many-electron wavefunction in the multidimensional configuration space, has gained wide acceptance (Popelier and Bultinck, 2009).

The charge density of an atom is given by

$$\begin{aligned}
 n(\mathbf{r}) &= \sum_{nlm} f_{nlm} |\psi_{nlm}(r, \theta, \phi)|^2 = \sum_{nlm} f_{nlm} |R_{nl}(r) Y_l^m(\theta, \phi)|^2 \\
 &= \sum_{n=0}^{n_{max}} \sum_{l=0}^{n-1} \sum_{m=-l}^l f_{nlm} R_{nl}^2(r) |Y_l^m(\theta, \phi)|^2 \\
 &= \sum_{n=0}^{n_{core}} \sum_{l=0}^{n-1} \sum_{m=-l}^l f_{nlm} R_{nl}^2(r) |Y_l^m(\theta, \phi)|^2 + \sum_{n=n_{core}+1}^{n_{max}} \sum_{l=0}^{n-1} \sum_{m=-l}^l f_{nlm} R_{nl}^2(r) |Y_l^m(\theta, \phi)|^2 \\
 &= \sum_{n=0}^{n_{core}} \sum_{l=0}^{n-1} f_{nl} R_{nl}^2(r) \left( \sum_{m=-l}^l |Y_l^m(\theta, \phi)|^2 \right) + \sum_{n=n_{core}+1}^{n_{max}} \sum_{l=0}^{n-1} \sum_{m=-l}^l f_{nlm} R_{nl}^2(r) |Y_l^m(\theta, \phi)|^2 \\
 &= \sum_{n=0}^{n_{core}} \sum_{l=0}^{n-1} f_{nl} R_{nl}^2(r) \left( \sum_{m=-l}^l |Y_l^m(\theta, \phi)|^2 \right) + \sum_{i=N_{core}+1}^{N_{occ}} f_i |\psi_i(\mathbf{r})|^2 \\
 &= n_{core}(\mathbf{r}) + n_{val}(\mathbf{r})
 \end{aligned} \tag{3}$$

where  $f_{nlm}$  is the occupancy of atomic orbital  $\psi_{nlm}(r, \theta, \phi)$ . We have split the density into core and valence parts, as shown in equation (3). As the core subshells are fully occupied, the occupancies  $\psi_{nlm}(r, \theta, \phi)$  are the same for each value of  $m$ , so that in equation (3) we replace  $f_{nlm}$  with  $f_{nl}$  for the core orbitals. As a result, we can apply the Spherical harmonic addition theorem :

$$\sum_{m=-l}^l Y_l^m(\theta, \phi) Y_l^m(\theta, \phi) = \frac{2l+1}{4\pi} \quad (4)$$

to obtain the following form for the core charge density

$$n_{core}(\mathbf{r}) = \sum_{n=0}^{n_{core}} \sum_{l=0}^{n-1} f_{nl} (2l+1) \frac{R_{nl}^2(r)}{4\pi} \quad (5)$$

But the spin up and down are treated equally so the coefficients  $f_{nl}$  have to be multiplied by 2 giving the final equation for the core charge density in the atom

$$n_{core}(\mathbf{r}) = \sum_{n=0}^{n_{core}} \sum_{l=0}^{n-1} f_{nl} 2(2l+1) \frac{R_{nl}^2(r)}{4\pi} = \frac{1}{4\pi} \sum_{nl} f'_{nl} R_{nl}^2(r) \quad (6)$$

where  $f'_{nl} = 2(2l+1)f_{nl}$ .

## 5. Calculations

Ab initio quantum chemical calculations were carried out to obtain the necessary electron densities.

### 5.1 Valence density $n_{val}(\mathbf{r})$ .

For the valence density, the calculation was made using ONETEP (Skylaris et al., 2005)(Order-N Electronic Total Energy Package), which is a linear-scaling code for quantum mechanical calculations based on Density Functional Theory being used to get the density  $n(\mathbf{r})$ . Since ONETEP uses norm-conserving ab initio pseudopotentials, the density is a coreless density and considered as a valence density  $n_{val}(\mathbf{r})$ :

$$n(\mathbf{r}) = n_{val}(\mathbf{r}) \quad (7)$$

### 5.2 Core density $n_{core}(\mathbf{r})$ .

The erratic behavior of the PP electronic density appears to be the main reason for the difficulties encountered in the topological analysis of such densities. One possibility of solving this problem lies in the addition of single-atom AE core density  $n_{core}(\mathbf{r})$  to the coreless density  $n_{val}(\mathbf{r})$  obtained in a pseudopotential calculation to get an augmented density  $n_{aug}(\mathbf{r})$  made up of:

$$n_{aug}(\mathbf{r}) = n_{core}(\mathbf{r}) + n_{val}(\mathbf{r}) \quad (8)$$

In principle, it would be better to use the core density obtained by numerically solving the atomic Hartree-Fock or Dirac-Fock equation, because they are used to fit pseudopotentials. Therefore, the core density generated in an independent atomic calculation: first the AE wavefunctions for the core electron of the neutral atom or the corresponding ion being calculated using OPIUM code (Opium, n.d.), which is also used to generate Hartree-Fock pseudopotentials that are used in the ONETEP code to get the PP density. Then a FORTRAN program CoRe (Core Reconstruct) is written to calculate the atomic core density using equation (6). Thus, the core densities  $n_{core}(\mathbf{r})$  of the atoms were obtained.

### 5.3 Augmented density $n_{aug}(\mathbf{r})$ .

The FORTRAN program CoRe is used to add the core density  $n_{core}(\mathbf{r})$  to the valence density  $n_{val}(\mathbf{r})$  to obtain the augmented density for isolated atom  $n_{aug}(\mathbf{r})$ . Using equation (6), the molecule augmented density  $n_{aug_m}(\mathbf{r})$  can be obtained, which is the sum of the augmented atomic densities  $n_{aug}(\mathbf{r})$  of the molecule components.

$$\begin{aligned} n_{aug_m}(\mathbf{r}) &= \sum_{k=1}^{n_{atom}} n_{aug_k}(\mathbf{r} - \mathbf{r}_k) \\ &= \sum_{k=1}^{n_{atom}} n_{core_k}(\mathbf{r} - \mathbf{r}_k) + n_{val_k}(\mathbf{r} - \mathbf{r}_k) \end{aligned} \quad (9)$$

where  $\mathbf{r}_k$  is the atomic position of atom  $k$

## 6. Results

## 6.1 Charge density

As mentioned earlier, one of the principal disadvantages of pseudopotential density is the absence of the contribution of core electron density. Figure (1) shows the difference between  $n_{val}(\mathbf{r})$ ,  $n_{aug}(\mathbf{r})$  and  $n_{core}(\mathbf{r})$  derived from electron density of nitrogen atom in alanine molecule.

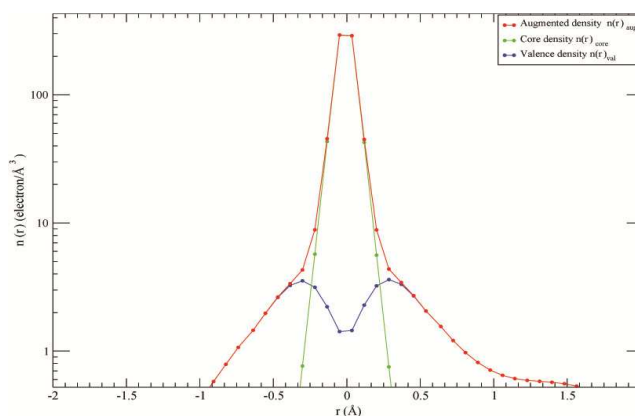
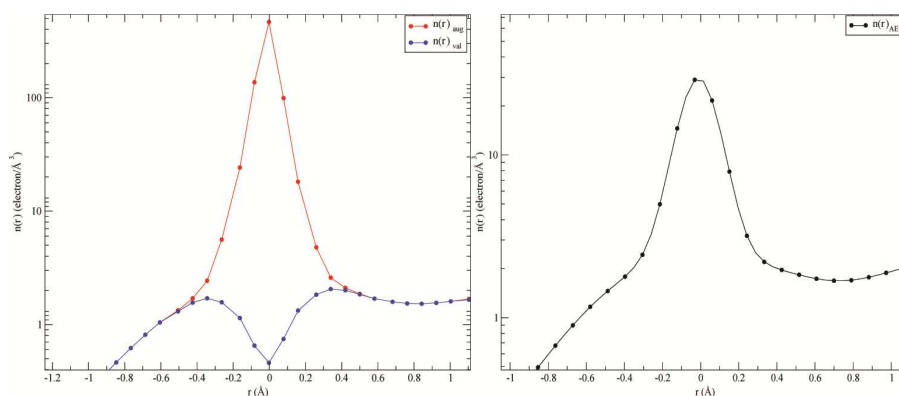


Figure 1 electron density versus distance from nucleus for nitrogen atom in Alanine

As expected, pseudopotential density  $n_{val}(\mathbf{r})$  displays a smoothed local minimum at the nucleus. Conversely,  $n_{aug}(\mathbf{r})$  density exhibits a very distinct maximum at the nucleus. The densities  $n_{val}(\mathbf{r})$  and  $n_{aug}(\mathbf{r})$  behave differently up to  $r = 0.5 \text{ \AA}$ , and this area penetrates deeply into the chemically interesting region.  $n_{val}(\mathbf{r})$  has a maximum at  $r = 0.28 \text{ \AA}$  in 3D space this corresponds to a continuum of degenerate (1,-1) critical points. A perturbation such as the presence of another atom eliminates the degeneracy and results in a set of (3,-1), and (3,-3) critical points. Thus, in a molecule there would be an unpredictable number of such critical points close to the nucleus. The behavior of the internuclear region within the framework of topological analysis of charge density is of particular interest. Hence, the spurious topology of  $n_{val}(\mathbf{r})$  in nuclear region does not necessarily affect the results. However, the existence of the appropriate (3,-1) critical point in  $n_{val}(\mathbf{r})$  between chemically bound atoms depends on whether the expected critical point belongs to the ascending or descending part of  $n_{val}(\mathbf{r})$ . shown in Figure 1.

Consider the augmented density obtained by the addition of core density to pseudopotential density and the all-electron density for the carbon atom in propanone. Figure 2 a displays electron density distribution in logarithmic scale for  $n_{val}(\mathbf{r})$ , and augmented density  $n_{aug}(\mathbf{r})$ . Figure 2 b displays all-electron density. At the nucleus the smoothed local minimum of  $n_{val}(\mathbf{r})$  is replaced by a very distinct maximum and results a (3,-3) critical point. The maximum of  $n_{val}(\mathbf{r})$  at  $r = 0.33 \text{ \AA}$  which corresponds to a continuum of degenerate (1,-1) critical points in pseudopotential density  $n_{val}(\mathbf{r})$  have been vanished. Thus, a significant improvement is achieved by using  $n_{aug}(\mathbf{r})$  instead of  $n_{val}(\mathbf{r})$ .



(a)  $n_{val}(\mathbf{r})$  density obtained from pseudopotential calculation ,and  $n_{aug}(\mathbf{r})$  addition of core density to pseudopotential density  
 (b)  $n_{AE}(\mathbf{r})$  all-electron density

Figure 2 Electron density versus the distance from the nucleus for carbon (C 1) atom in Propanone ((CH<sub>2</sub>)CO).

Figure (3) shows density distribution between carbon(C 1) and carbon(C 2) atom in ethene(C<sub>2</sub>H<sub>4</sub>). For all-electron density  $n_{AE}(\mathbf{r})$  a pattern typical for two atoms connected by a chemical bond obtained. It contains two sharp maxima located at the nuclei and a saddle point that corresponds to (3,-1) bond critical point in 3D space for all-electron density distribution. The pseudopotentials density  $n_{val}(\mathbf{r})$  obtained using pseudopotentials for same atoms is completely different. There is no (3,-1) critical point between C1 and C2 atom. Therefore, it is reasonable to suppose that the lack of core density gives rise to the absence of bond critical point. The failure of PP density to reproduce carbon-carbon bond critical points can be corrected by adding atomic core density to pseudopotentials density . Figure (3) also shows the density distribution between carbon and carbon atoms in ethene (C<sub>2</sub>H<sub>4</sub>) for  $n_{aug}(\mathbf{r})$  density. The shape of  $n_{aug}(\mathbf{r})$  is qualitatively identical to  $n_{AE}(\mathbf{r})$  . Sharp maxima at the nuclei are separated by a(3,-1) critical point.  $n_{aug}(\mathbf{r})$  is quite close to  $n_{AE}(\mathbf{r})$  except for a small interval.

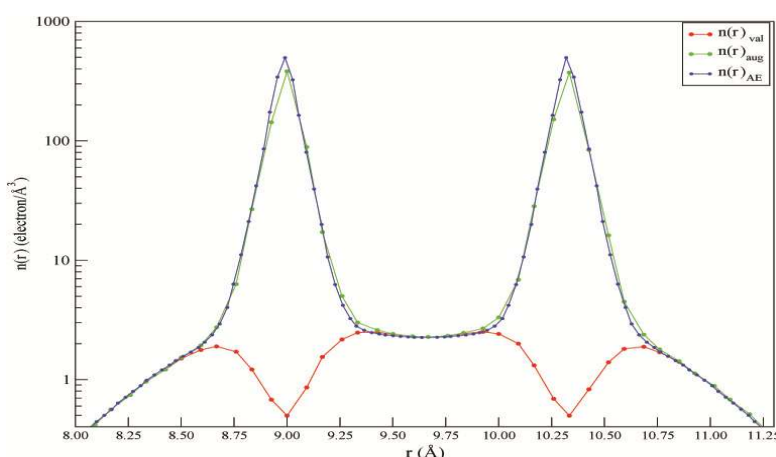


Figure 3 Electron density versus distance from nucleus of carbon (C 1) carbon (C 2) atom in ethene (C<sub>2</sub> H<sub>4</sub> ).

## 6.2 Bader analysis

In order to quantify the effect of core electron absences in topological analysis of charge density, a Bader analysis has been performed using Henkelman code (Henkelman, Arnaldsson and J, 2006)the analysis include all-

electron, valence, and augmented density.

Valence density of ethene has been obtained using ONETEP code using the kinetic energy cutoff of 2000 eV, for carbon atoms the normconserving pseudopotentials has been used while for hydrogen a pure Coulomb potential has been used to see the cusp corrections in action. For all-electron density (Windus et al., 2003) code has been used, Gaussian basis sets with the use of the triple-split valence basis 6-311G\*\* has been used for carbon and hydrogen.

Calculation for aminophenol valence density has been performed using ONETEP with kinetic energy cutoff of 2000 eV, , again for carbon, oxygen, nitrogen atoms, normconserving pseudopotentials has been used and for hydrogen a pure Coulomb potential has been used. For all-electron density Nwchem code has been used, Gaussian basis sets with the use of the triple-split valence basis 6-311G\*\* for all atoms.

Propanone valence density obtained using ONETEP code with 2000 eV cutoff energy and normconserving pseudopotentials has been used carbon, oxygen, nitrogen atoms the and for hydrogen a pure Coulomb potential. Nwchem code using Gaussian basis sets with the use of the triple-split valence basis 6-311G\*\* for all atoms.

The intial significant improvement in valence density by adding core density and constructing augmented density is the number of electrons and number of significant maxima in density of a molecule. Table 2 shows this improvement for different molecules. Number of electrons for valence density calculation show the missing of core electron (the core electrons have been treated within the framework of pseudopotentials) and reprot the total number of valence electron, while augmented density calculation Leds to addition of core electron to valence and produce correct total number of electrons which can be ea sly noted compared to total number of electrons for all electron density calculations. More accurate total number of electron can be achieved using a fine grid box in calculation but then segmentation fault problems arise with the the Henkelman code .

Table 3 shows the number of significant maxima in density, again the augmented density shows the improvement achieved by the core electrons addition to the valence density. In general, number of significant maxima of valence density are larger (about two times) than all-electron and augmented density and this is expected due to the fact that in a molecule there would be unpredictable number of (3,-1), and (3,-3) critical points close to the nucleus. Adding core electron density to valence density participate in the elimination of the maximas close to nucleus and produce a single sharpe local maxi ma. As a result number of significant maxima of augmented density give identical value to all-electron density so that the Bader code will correctly identify the maximas and produce the correct Bader volumes.

Table 2 Number of Electrons

Molecule	All-electron density	Augmented density	Valence density
Propanone	31.9	32.0	24.0
Ethene	15.9	15.9	11.9
Aminophenol	57.9	58.0	42.0

Table 3 Significant Maxima

Molecule	All-electron density	Augmented density	Valence density
Propanone	10	10	18
Ethene	6	6	10
Aminophenol	15	15	31

Bader defines the atomic charges as integrals over Bader volumes  $\Omega_n(\mathbf{r})$ . Each Bader volume contains a single electron density maximum and is separated from other volumes by a zero flux surface of the gradients of the electron density, Each volume  $\Omega_n(\mathbf{r})$  is defined by a set of points where following a trajectory of maximizing  $n(\mathbf{r})$  reaches the same unique maximum (fixed point).

Figure 6 shows Bader's volume for ethene molecule (Fig 5), Bader's volume with sharp boundaries between atoms in bonding regions, identical atomic volumes for both carbon and hydrogen atoms with very smooth volume boundaries for the all-electron density (Fig 6c), valence density (Fig 6b) and augmented (Fig 6a) Bader's volume are with rough boundaries between atoms in bonding regions. Overall, good agreement is obtained between augmented and all-electron density.

The charge enclosed within the Bader volume is a good approximation to the total electronic charge of an atom, table (4) report the Bader analysis electronic charge of atoms for ethene using both Voronoi and Bader charge analysis scheme.

The most striking result to emerge from the data is that a significant improvement in atomic charge for ethene atoms using core electron density addition to valence density, for carbon atoms using Bader charge analysis scheme results (Table (4)) shows an excellent agreement between augmented and all-electron atomic charge compared with valence density atomic charge, the effect of core electron can be clearly shown from the values of carbon atomic charge, for example, carbon (C 1) charge from valence density Bader results report 4.0482 electron while all-electron density report 6.0730 electron since the core electrons have been treated within the framework of pseudopotentials this difference is expected, augmented density atomic charge report 6.0502 electron for C 1 and this a strong evidence of core electron improvement of valence density if the atomic charge compared to all-electron density. Hydrogen atomic charges for all densities in general is in good agreement due to the fact that hydrogen atom has been treated using a pure Coulomb potential in DFT calculation to get valence density and that insure to have the correct atomic charge. In general, the Voronoi charge is differ from the Bader charge due to the the fact that Voronoi charges are based on dividing the physical space according to a distance criterion, i.e. a given point in space belongs to the nearest nucleus, and again the augmented density atomic charge confirm the effect of the core electron when compared to all-electron and valence density.

For aminophenol molecule (Fig. 7) the Bader's volume boundaries between atoms shown in Fig 8c, boundaries between atoms in bonding regions between all atoms for the all-electron density (Fig 8c), augmented (Fig 8a), and valence density (Fig 8b). The results, indicate that augmented density atomic charge using Bader charge analysis scheme shows improvement as compared to all-electron density atomic charge and this can be clearly shown from the smooth in Bader's volume boundaries between C 1 and O 1, for all-electron volumes shows straight cut (a plane perpendicular to the bond between them) and that has been achieved in augmented density, while for valence density there is a curved line border between those two volumes and this means that a part of carbon (C 1) atomic charge been emerged into oxygen (O 1) atomic volume, this can be highlighted from the atomic charge of each atom in table (5) for C 1 atom the atomic charges is 5.0633 electron from all-electron density and 5.1708 electron for augmented density, while the valence density atomic charge is 2.3160 electron which is too small compare to all-electron and augmented densities, and it is clear that after adding the core electron the the correct atomic charge partition has been made between these two atoms and the atomic charge become in good agreement.

Atomic charge density for propanone molecule (Fig. 9) show a very good example on the effect of core electron on the correct partition between atom in molecule using Bader analysis, figure( 10 ) shows the Bader's volumes of atoms between carbon (C 2) and oxygen (O 1) atoms, similarity can be easily noted between all-electron (fig 10c) and augmented density (fig 10a), atomic charge volumes with straight cut in Bader's volume boundaries and the curved line border with the valence density (fig 10b) atomic charge volumes, again this can be highlighted from the atomic charge of each atom in Table (6) for C 2 atom the atomic charges is 5.5266 electron from all-electron density and 5.6748 electron for augmented density, while the valence density atomic charge is 3.1642 electron and it is clear that after adding the core electron the the correct atomic charge partition has been made between these two atoms and the atomic charge become in good agreement, this can be more clear from the oxygen (O 1) atomic charge there is an excellent agreement between augmented and all-electron atomic charge compared with valence density atomic charge, although the valence density atomic charge is 7.8049 electron and the core electron augmentation should increase the atomic charge by 2.00 electron as a result a atomic charge of 9.8049 electron belong to oxygen in propanone molecule but the correct volume partition of charge in molecule produced by the correct of the density topology from pseudopotential by adding the core electron density leads to the excellent agreement between augmented and all-electron atomic charge.

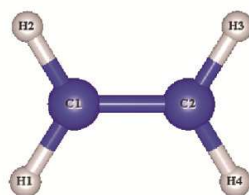


Figure 4 Ethene ( $C_2H_4$ ).

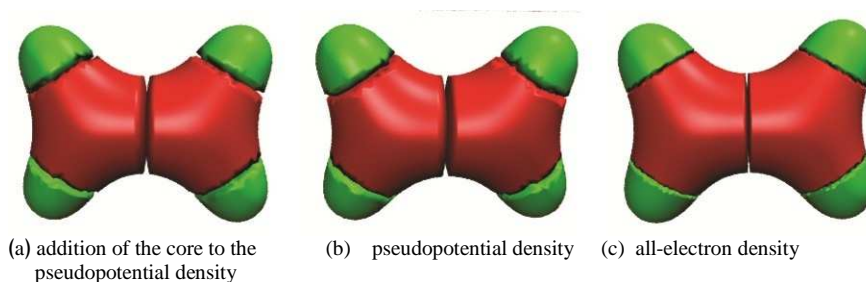


Figure 5 Bader Volumes of Ethene ( $C_2H_4$ ) atoms.

Table 4 Atomic Charge of Bader's Volume for Ethene atoms

Atom	All-electron Density		Augmented Density		Pseudopotential Density	
	Bader	Voronoi	Bader	Voronoi	Bader	Voronoi
C 1	6.0730	5.0513	6.0502	4.9844	4.0482	2.9827
C 2	6.0730	5.0514	6.2242	5.1388	4.1681	3.1406
H 1	0.9630	1.4738	0.9327	1.4659	0.9327	1.4658
H 2	0.9630	1.4738	0.9349	1.4675	0.9349	1.4674
H 3	0.9630	1.4738	0.9385	1.4693	0.9391	1.4692
H 4	0.9630	1.4738	0.9200	1.4746	0.9770	1.4744

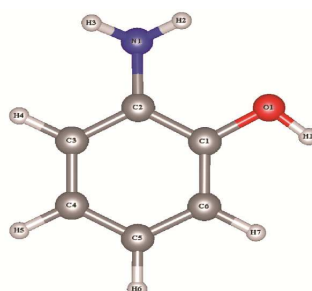


Figure 6 Aminophenol ( $C_6H_7NO$ ).

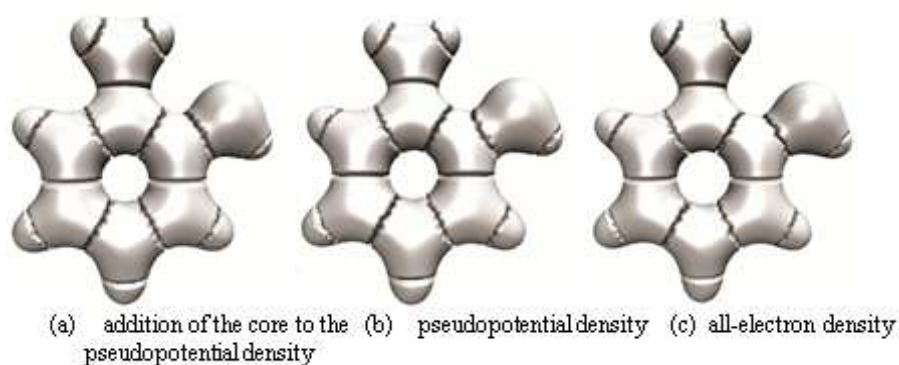


Figure 7 Bader Volumes of Aminophenol (C<sub>6</sub>H<sub>5</sub>(OH)NH<sub>2</sub>) atoms.

Table 5 Atomic Charge of Bader's Volume for Aminophenol atoms

Atom	All-electron Density		Augmented Density		Pseudopotential Density	
	Bader	Voronoi	Bader	Voronoi	Bader	Voronoi
C 1	5.5266	5.8272	5.6748	5.9251	3.1642	3.8463
O 1	9.0367	7.7244	9.1606	7.8394	7.5270	5.7727
C 2	5.6538	5.8688	5.7058	5.8944	3.6869	3.8825
N 1	8.0324	6.1391	8.1009	6.1622	6.1160	4.1708
C 2	6.0759	5.5662	6.1695	5.5306	4.1827	3.5449
C 3	5.9702	5.5025	5.9498	5.5261	3.9796	3.5570
C 4	6.0524	5.5657	6.1329	5.5468	4.1412	3.5562
C 5	6.1150	5.5592	6.0001	5.4962	4.0346	3.5310
H 1	0.4007	1.3831	0.3591	1.3807	0.3591	1.3806
H 2	0.5925	1.4504	0.5517	1.4448	0.5517	1.4447
H 3	0.6095	1.4420	0.5788	1.4332	0.5788	1.4331
H 4	0.9530	1.4780	0.9224	1.4704	0.9232	1.4703
H 5	0.9814	1.4827	0.9139	1.4776	0.9146	1.4775
H 6	0.9897	1.4851	0.8835	1.4651	0.8835	1.4650
H 7	0.9604	1.4758	0.9564	1.4676	0.9570	1.4675

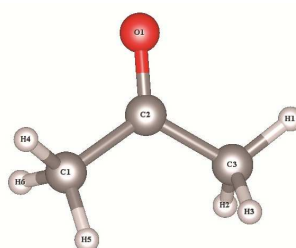


Figure 7 Propanone ((CH<sub>3</sub>)<sub>2</sub>CO).

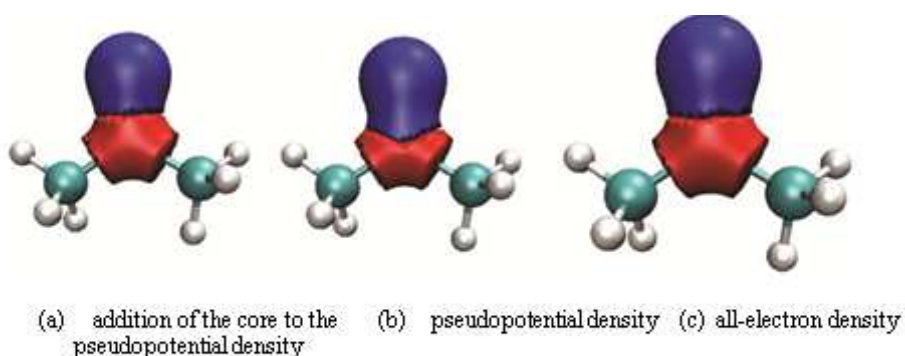


Figure 9 Bader Volumes of C 2 and O 1 of Propanone ((CH<sub>3</sub>)<sub>2</sub>CO).

Table 6 Atomic Charge of Bader's Volume for Propanone atoms

Atom	All-electron Density		Augmented Density		Pseudopotential Density	
	Bader	Voronoi	Bader	Voronoi	Bader	Voronoi
C 1	6.1239	4.6414	5.3981	4.7089	4.1669	2.6764
C 2	5.0633	5.6338	5.1708	5.6277	2.3160	3.6356
O 1	8.9314	8.3054	8.9065	8.3686	7.8049	6.4038
C 3	6.1073	4.6715	5.3724	4.7149	4.2080	2.6748
H 1	0.9784	1.4459	0.9891	1.4335	0.8941	1.4334
H 2	0.9418	1.4446	0.9845	1.4347	0.8950	1.4346
H 3	0.9514	1.4446	0.9986	1.4353	0.9304	1.4352
H 4	0.9223	1.4408	0.9813	1.4299	0.9107	1.4297
H 5	0.9576	1.4582	0.9859	1.4497	0.9652	1.4496
H 6	0.9464	1.4376	0.9976	1.4269	0.9088	1.4268

## 7. Conclusions

In this report it has been attempted to analyze the effect of core electrons density on topological analysis of density. It has been shown that pseudopotential density (valence density) is the main reason for the difficulties encountered in the topological analysis of such densities within the Bader quantum theory of atoms in molecules (QTAIM). We have here described a method to by pass the erratic behavior of the pseudopotential electronic density that is considered appropriate to perform topological analysis of such densities. We have found significant evidence that the core density addition is capable to reconstruct the correct topology of density from pseudopotential calculations. Comparison between all-electron and augmented density results from Bader analysis are in excellent agreement. We have obtained accurate results proving that the augmented density can be used in topological analysis of density.

## References

- Bader, R.F.W. (1994) *Atoms in molecules: a quantum theory*, Clarendon Press, Available: <http://books.google.com/books?id=tyVpQgAACAAJ>.
- Cioslowski, J. and Piskorz, P. (1996) 'Properties of atoms in molecules from valence-electron densities augmented with core-electron contributions', *Chemical Physics Letters*, vol. 255, no. 4-6, pp. 315-319, Available: <http://www.sciencedirect.com/science/article/pii/0009261496004046>.
- de-la Roza, A.O., Blanco, M.A., Pendas, A.M. and Luana, V. (2009) 'Critic: a new program for the topological analysis of solid-state electron densities', *Computer Physics Communications*, vol. 180, no. 1, pp. 157-166, Available: HYPERLINK "<http://www.sciencedirect.com/science/article/pii/S0010465508002865>"
- Fonseca Guerra, C., Handgraaf, J.-W., Baerends, E.J. and Bickelhaupt, F.M. (2004) 'Voronoi deformation density (VDD) charges: Assessment of the Mulliken, Bader, Hirshfeld, Weinhold, and VDD methods for charge analysis', *Journal of Computational Chemistry*, vol. 25, no. 2, pp. 189-210, Available: HYPERLINK "<http://dx.doi.org/10.1002/jcc.10351>" <http://dx.doi.org/10.1002/jcc.10351>.
- Francl, M.M. and Chirlian, L.E. (2007) 'The Pluses and Minuses of Mapping Atomic Charges to Electrostatic Potentials', in *Reviews in Computational Chemistry*, John Wiley & Sons, Inc., Available: <http://dx.doi.org/10.1002/9780470125915.ch1>.
- Henkelman, G., Arnaldsson, A. and J (2006) 'A fast and robust algorithm for Bader decomposition of charge density', *Computational Materials Science*, vol. 36, no. 3, pp. 354-360, Available: HYPERLINK "<http://www.sciencedirect.com/science/article/pii/S0927025605001849>"
- Hirshfeld, F.L. (1977) 'Bonded-atom fragments for describing molecular charge densities', *Theoretical Chemistry Accounts: Theory, Computation, and Modeling (Theoretica Chimica Acta)*, vol. 44, pp. 129-138, Available: HYPERLINK "<http://dx.doi.org/10.1007/BF00549096>"
- Jensen, F. (2006) *Introduction to Computational Chemistry*, 2<sup>nd</sup> edition, Wiley, Available: <http://www.worldcat.org/isbn/0470011874>.
- Katan, C., Rabiller, P., Lecomte, C., Guezo, M., Oison, V. and Souhassou, M. (2003) 'Numerical computation of critical properties and atomic basins from three-dimensional grid electron densities', *Journal of Applied Crystallography*, vol. 36, no. 1, pp. 65-73, Available: HYPERLINK "<http://dx.doi.org/10.1107/S0021889802018691>"
- L.A., P. and Popelier (1996) 'MORPHY, a program for an automated atoms in molecules analysis', *Computer Physics Communications*, vol. 93, no. 2-3, pp. 212-240, Available: HYPERLINK "<http://www.sciencedirect.com/science/article/pii/0010465595001131>"
- Mulliken, R.S. (1955) 'Electronic Population Analysis on LCAO-MO Molecular Wave Functions. I', vol. 23, no. 10, pp. 1833-1840, Available: HYPERLINK "<http://dx.doi.org/doi/10.1063/1.1740588>"
- Opium (n.d) 'Opium - pseudopotential generation project', Available: HYPERLINK "<http://opium.sourceforge.net/>"
- Phillips, J.C. and Kleinman, L. (1959) 'New Method for Calculating Wave Functions in Crystals and Molecules', *Phys. Rev.*, vol. 116, Oct, pp. 287-294, Available: HYPERLINK "<http://link.aps.org/doi/10.1103/PhysRev.116.287>"
- Popelier, P. and Bultinck, P. (2009) 'Atoms in Molecules and Population Analysis' CRC Press.
- Rousseau, B., Peeters, A. and Alsenoy, C.V. (2001) 'Atomic charges from modified Voronoi polyhedra', *Journal of Molecular Structure: THEOCHEM*, vol. 538, no. 1-3, pp. 235-238, Available: HYPERLINK "<http://www.sciencedirect.com/science/article/pii/S0166128000006928>"
- Skyllaris, C.-K., Haynes, P.D., Mostofi, A.A. and Payne, M.C. (2005) 'Introducing ONETEP: Linear-scaling density functional simulations on parallel computers', vol. 122, no. 8, p. 084119, Available: HYPERLINK "<http://dx.doi.org/doi/10.1063/1.1839852>"
- Stephane, N., Krokidis, X., Fuster, F. and Silvi, B. (1999) 'Computational tools for the electron localization function topological analysis', *Computers & Chemistry*, vol. 23, no. 6, pp. 597-604, Available: HYPERLINK "<http://www.sciencedirect.com/science/article/pii/S009784859900039X>"
- Vyboishchikov, S.F., Sierraalta, A. and Frenking, G. (1997) 'Topological analysis of electron density distribution taken from a pseudopotential calculation', *Journal of Computational Chemistry*, vol. 18, no. 3, pp. 416-429, Available: HYPERLINK "[http://dx.doi.org/10.1002/\(SICI\)1096-987X\(199702\)18:3%3c416::AID-](http://dx.doi.org/10.1002/(SICI)1096-987X(199702)18:3%3c416::AID-)

---

JCC11%3e3.0.CO;2-G" [http://dx.doi.org/10.1002/\(SICD\)1096-987X\(199702\)18:33.0.CO;2-G](http://dx.doi.org/10.1002/(SICD)1096-987X(199702)18:33.0.CO;2-G).  
Windus, T., Bylaska, E., Dupuis, M., Hirata, S., Pollack, L., Smith, D., Straatsma, T. and Apr (2003) 'NWChem: New Functionality', in Sloot, P., Abramson, D., Bogdanov, A., Gorbachev, Y., Dongarra, J. and Zomaya, A. (ed.) *Computational Science ICCS 2003*, Springer Berlin / Heidelberg.

This academic article was published by The International Institute for Science, Technology and Education (IISTE). The IISTE is a pioneer in the Open Access Publishing service based in the U.S. and Europe. The aim of the institute is Accelerating Global Knowledge Sharing.

More information about the publisher can be found in the IISTE's homepage:

<http://www.iiste.org>

## CALL FOR JOURNAL PAPERS

The IISTE is currently hosting more than 30 peer-reviewed academic journals and collaborating with academic institutions around the world. There's no deadline for submission. **Prospective authors of IISTE journals can find the submission instruction on the following page:** <http://www.iiste.org/journals/> The IISTE editorial team promises to review and publish all the qualified submissions in a **fast** manner. All the journals articles are available online to the readers all over the world without financial, legal, or technical barriers other than those inseparable from gaining access to the internet itself. Printed version of the journals is also available upon request of readers and authors.

## MORE RESOURCES

Book publication information: <http://www.iiste.org/book/>

Recent conferences: <http://www.iiste.org/conference/>

## IISTE Knowledge Sharing Partners

EBSCO, Index Copernicus, Ulrich's Periodicals Directory, JournalTOCS, PKP Open Archives Harvester, Bielefeld Academic Search Engine, Elektronische Zeitschriftenbibliothek EZB, Open J-Gate, OCLC WorldCat, Universe Digital Library, NewJour, Google Scholar

